

# Synthesis and properties of sulfonated copoly(*p*-phenylene)s containing aliphatic alkyl pendant for fuel cell applications

Surasak Seesukphronrarak, Kayo Ohira, Koh Kidena, Naohiko Takimoto, Carlos Seiti Kuroda, Akihiro Ohira\*

FC-Cubic, National Institute of Advanced Industrial Science and Technology (AIST), Tokyo 135-0064, Japan

## ARTICLE INFO

### Article history:

Received 5 October 2009  
Received in revised form  
18 December 2009  
Accepted 21 December 2009  
Available online 4 January 2010

### Keywords:

Polymer electrolyte membrane  
Dimensional stability  
Proton conductivity

## ABSTRACT

A series of novel copoly(*p*-phenylene)s (PPs) containing an alkyl pendant were successfully synthesized via Ni(0)-catalyzed coupling polymerization. Sulfonated copolymers (SPPs) were achieved by postsulfonation from concentrated H<sub>2</sub>SO<sub>4</sub>. SPPs showed good solubility in polar aprotic solvents and gave flexible, tough, and transparent free-standing films by solvent casting. The ion exchange capacities (IECs) of the membranes ranged from 2.50 to 2.65 meq/g. All SPP membranes displayed proton conductivity similar to or higher than that of Nafion, especially at high relative humidity (>70% RH) (SPP-1: 0.271 Scm<sup>-1</sup>, SPP-2: 0.284 Scm<sup>-1</sup>, SPP-3: 0.212 S cm<sup>-1</sup>, Nafion: 0.127 Scm<sup>-1</sup>; at 80 °C and 95% RH). They also exhibited acceptable water uptake in the range of 52–56 vol% at 80 °C with little dimensional change. The gas permeability of the SPP membranes was much lower than that of Nafion 112. Therefore, these materials are promising for fuel cell application.

© 2010 Elsevier Ltd. All rights reserved.

## 1. Introduction

In recent years, polymer electrolyte membranes (PEMs) have played an important role as a key component of polymer electrolyte fuel cells (PEFCs) for transport, stationary, and portable power sources. Among PEMs, the perfluorinated sulfonic acid (PFSA) ionomer introduced by DuPont under the registered trademark Nafion in 1966 is the current state-of-the-art PEM in commercial systems owing to its excellent mechanical properties, good chemical stability, and high proton conductivity. However, its high cost, high gas permeability, and relatively low conductivity at high temperatures have limited its widespread commercial and practical use in PEFCs [1–3]. Therefore, considerable effort has been devoted to developing an alternative proton-conductive membrane. To date, many types of sulfonated hydrocarbon (HC)-type ionomer membrane based on high-performance aromatic polymers, such as sulfonated polyimides [4–7], sulfonated poly(ether ketone)s [8–11], sulfonated poly(arylene ether sulfone)s [12–15], sulfonated poly-benzimidazoles [16], and sulfonated poly(*p*-phenylene)s [17–21], have been extensively developed as candidate PEM materials. In general, the HC-type ionomer membrane is considered to offer greater structural and thermal stability than the PFSA ionomer

membrane. However, an HC-type ionomer membrane with a random copolymer system needs to have a high IEC to achieve high proton conductivity, as high as that of Nafion, resulting in unfavorable excess water swelling of the membrane and loss of physical properties. Some approaches that have been applied to solving these problems include the blending and cross linking of ionomer membranes [22–24], the radiation grafting of polymer membranes [25,26], and the development of multiblock copolymer membranes composed of sulfonated hydrophilic and non-sulfonated hydrophobic [27–30].

Recently, investigations of sulfonated poly(*p*-phenylene)s, containing sulfonic acid groups on flexible pendant side chains, and their derivatives have received much attention as candidate PEFC materials owing to their excellent thermal and hydrolytic stabilities, and high proton conductivities comparable to those of Nafion. McGrath et al., for example, reported a synthesis of sulfonated poly(2,5-benzophenone) and its derivative by nickel(0) catalytic coupling polymerization and followed by sulfonation with sulfuric acid or by substitution of activated fluoro groups in the polymers side chain. The resulting polymers showed good solubility in dipolar solvents but bad film-forming ability, probably owing to their rigid-rod backbone, which limit their industrial application in PEFCs [18]. Sulfonated poly(*p*-phenylene)s should have a high molecular weight for good handling and mechanical stabilities; however, there are only a few reports on sulfonated poly(*p*-phenylene)s with high molecular weights owing to the difficulty in the

\* Corresponding author. Tel.: +81 3 3599 8550; fax: +81 3 3599 8554.  
E-mail address: a-ohira@aist.go.jp (A. Ohira).

synthesis of such materials. On the basis of the above results, we have succeeded in the fabrication of membranes with good swelling control even with increasing water content, without obstructing the proton conduction as well as enhance membrane flexibility by introducing comonomer unit that possesses the long alkyl side chain in a random copolymer.

In the present work we have designed and prepared a series of sulfonated copoly(*p*-phenylene)s containing aliphatic alkyl pendant side chain by Ni(0) catalyzed coupling polymerization. Sulfonated poly(*p*-phenylene)s can be synthesized by postsulfonation from concentrated H<sub>2</sub>SO<sub>4</sub>. It is expected that the introduction of aliphatic alkyl side chain in copoly(*p*-phenylene)s backbones will result in good solubility in organic solvents, improved film-forming ability, good water stability, and high proton conductivity. The properties of the synthesized copolymer membranes such as solubility, IEC, water uptake, thermal stability, dimensional change, proton conductivity, and gas permeability were investigated.

## 2. Experimental

### 2.1. Materials

All reagents and solvent were purchased from Aldrich and used without further purification. Triphenylphosphine was purified by recrystallization from *n*-hexane. *N*-Methyl-2-pyrrolidinone (NMP, anhydrous grade from Aldrich) was also used as received. 2,5-Dichlorobenzoyl chloride was prepared from 2,5-Dichlorobenzoic acid with thionyl chloride (SOCl<sub>2</sub>). Sulfonation of PEEK was carried out using 96% H<sub>2</sub>SO<sub>4</sub> for 72 h according to a procedure reported elsewhere [31]

### 2.2. Characterization

Infrared spectra were recorded on a Varian FTS-7000 FT-IR spectrometer. <sup>1</sup>H and <sup>13</sup>C NMR spectra were obtained on JEOL ECA-500 using CDCl<sub>3</sub> as the solvent with tetramethylsilane as the internal reference. The molecular weight of the synthesized polymers were estimated by gel permeation chromatography (GPC) equipped with two consecutive columns (GF-7M HQ and GF-310 HQ, Asahipak) connected to a Shimadzu SPD-20AU UV detector at 40 °C using polystyrene standards and dimethylformamide containing 0.05 M LiBr as the eluent at a flow rate of 0.05 mL/min. UV-vis absorption spectra were measured with a Spectrometer (MCPD-7000, Otsuka Electronics Co., Ltd.) equipped with an optical fiber. Thermogravimetric analysis (TGA) was performed with the TGA-50 analyzer (Shimadzu). The polymer samples were dried at 100 °C prior to the experiments and heated from room temperature to 800 °C at a heating rate of 10 °C/min in nitrogen atmosphere (flow rate, 50 mL/min). Tensile measurement was achieved and analyzed at the Toray Research Center (Shiga, Japan) using Instron® Model 5848 Micro Tester (Instron Co., Ltd.). The test speed of 2 mm/min, the size of specimen is 15 mm × 4 mm. For each testing, three measurements at least were recorded and the average value was calculated.

### 2.3. Monomer synthesis

The monomers *M1*, *M2*, *M3*, and *M4* were prepared in one step by the Friedel-Crafts acylation of diphenylether, *n*-propylbenzene, *n*-dodecylbenzene, and *n*-octadecylbenzene, respectively, with 2,5-dichlorobenzoyl chloride according to a previously report with some modifications [32–34].

The general procedure for the preparation of monomers is as follows. A solution of aromatic substrate (1 eq) and 2,5-dichlorobenzoyl chloride (1.1 eq) in dichloromethane (5 eq) was charged into

a three-neck flask. The reaction mixture was cooled in an ice/water bath. Anhydrous AlCl<sub>3</sub> (1 eq) was added gradually to the reaction mixture whose temperature was kept below 10 °C. After adding all the AlCl<sub>3</sub>, the reaction solution was allowed to slowly warm to room temperature and stirred overnight. The reaction was stopped by pouring the solution into acidic ice water. The resulting two layers were separated and the organic layer was washed with 10% aqueous NaOH and water, and dried over MgSO<sub>4</sub>. After filtration, the solvent was removed and the residue was purified by column chromatography (CH<sub>2</sub>Cl<sub>2</sub>/hexane) or recrystallization.

#### 2.3.1. 2,5-dichloro-4-phenoxybenzophenone (*M1*)

From 2,5-dichlorobenzoyl chloride and diphenylether: White crystalline solid (yield 85%) <sup>1</sup>H NMR (500 MHz, CDCl<sub>3</sub>): δ(ppm) 7.77 (d, 2H), 7.41–7.37 (m, 4H), 7.33 (s, 1H), 7.20 (dd, 1H), 7.08 (dd, 2H), 6.99 (dd, 2H). <sup>13</sup>C NMR (100 MHz, CDCl<sub>3</sub>) δ 192.2, 163.1, 155.1, 140.2, 133.0, 132.6, 131.3, 131.0, 130.3, 130.2, 129.5, 128.8, 125.0, 120.6, 117.3.

#### 2.3.2. 2,5-dichloro-4-propylbenzophenone (*M2*)

From 2,5-dichlorobenzoyl chloride and *n*-propylbenzene: Colorless liquid (yield 90%) <sup>1</sup>H NMR (500 MHz, CDCl<sub>3</sub>): δ(ppm) 7.71 (d, 2H), 7.38 (s, 2H), 7.33 (s, 1H), 7.27 (d, 2H), 2.66 (t, 2H), 1.66 (q, 2H), 0.95 (t, 3H). <sup>13</sup>C NMR (100 MHz, CDCl<sub>3</sub>) δ 193.3, 149.9, 140.3, 133.6, 132.9, 131.3, 130.9, 130.3, 129.6, 128.9, 128.8, 38.3, 24.3, 13.9.

#### 2.3.3. 2,5-dichloro-4-dodecylbenzophenone (*M3*)

From 2,5-dichlorobenzoyl chloride and *n*-dodecylbenzene: light yellow liquid (yield 92%) <sup>1</sup>H NMR (500 MHz, CDCl<sub>3</sub>): δ(ppm) 7.70 (d, 2H), 7.38 (s, 2H), 7.33 (s, 1H), 7.28 (d, 2H), 2.68 (t, 2H), 1.63 (t, 2H), 1.25 (m, 18H), 0.87 (t, 3H). <sup>13</sup>C NMR (100 MHz, CDCl<sub>3</sub>) δ 193.3, 150.2, 140.3, 133.6, 132.9, 131.3, 130.9, 130.4, 129.6, 128.9, 36.3, 32.0, 31.1, 29.7, 29.6, 29.4, 22.8, 14.3.

#### 2.3.4. 2,5-dichloro-4-octadecylbenzophenone (*M4*)

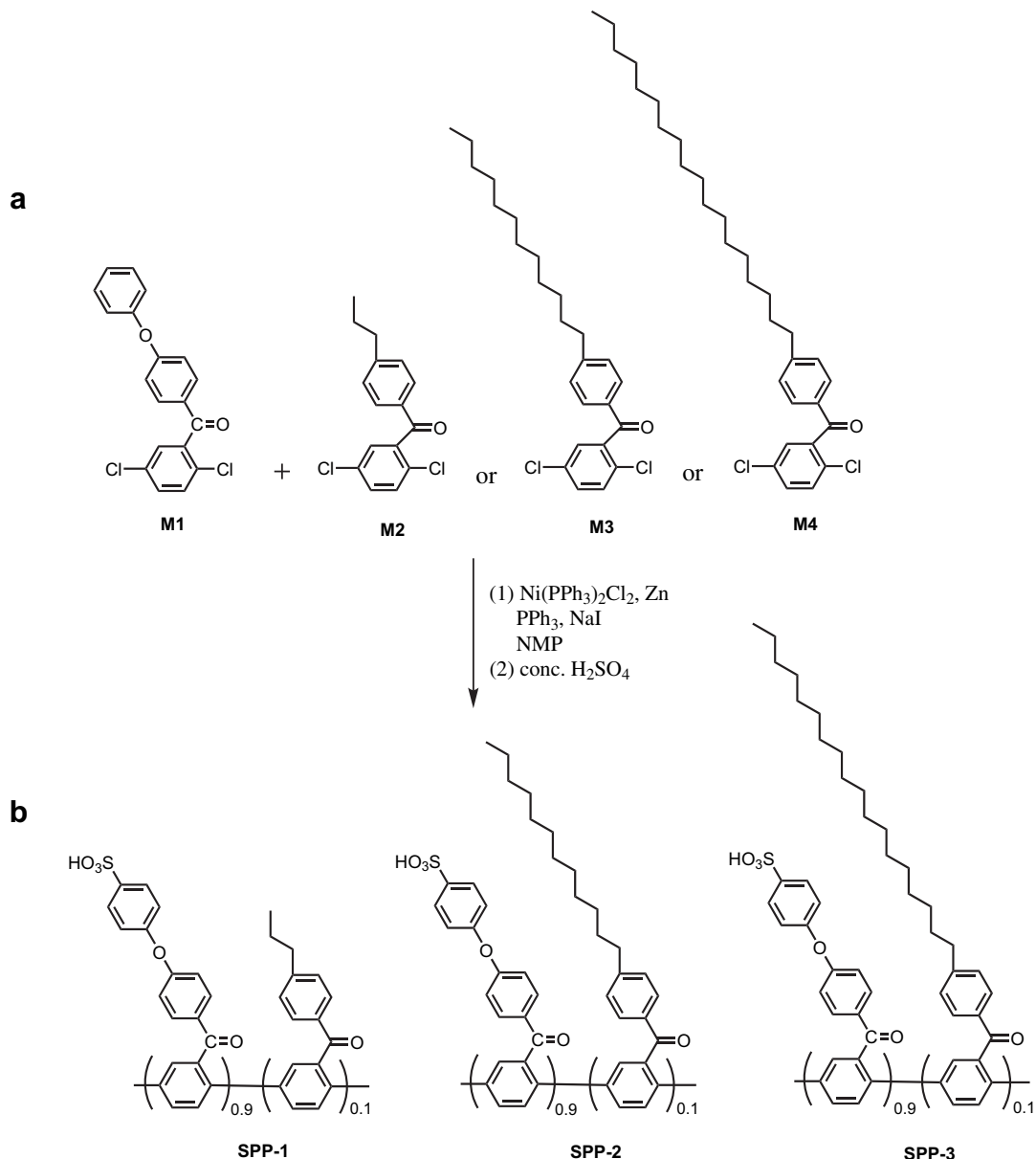
From 2,5-dichlorobenzoyl chloride and *n*-octadecylbenzene: Pale yellow semi-solid (yield 96%) <sup>1</sup>H NMR (500 MHz, CDCl<sub>3</sub>): δ(ppm) 7.71 (d, 2H), 7.38 (s, 2H), 7.33 (s, 2H), 7.25 (d, 2H), 2.67 (t, 2H), 1.63 (t, 2H), 1.25 (m, 30H), 0.87 (t, 3H). <sup>13</sup>C NMR (100 MHz, CDCl<sub>3</sub>) δ 193.3, 150.2, 140.3, 133.6, 132.9, 131.2, 130.9, 130.3, 129.6, 128.9, 36.3, 32.0, 31.1, 29.8, 29.6, 29.5, 29.4, 22.8, 14.2.

## 2.4. Polymerization of poly(*p*-phenylene)s (PPs)

As shown in Scheme 1, polymers were synthesized via Ni(0) catalytic polymerization according to a procedure described in previous reported with some modification [32,33] A typical example of polymerization is as follows. In a 100-mL three-neck round-bottom flask, Ni(PPh<sub>3</sub>)<sub>2</sub>Cl<sub>2</sub> (0.122 g, 0.186 mmol), Zn (0.654 g, 10 mmol), PPh<sub>3</sub> (0.524 g, 2 mmol), and NaI (0.088 g, 0.058 mmol) were charged into a flask under argon atmosphere. Dry NMP (6 mL) was added to the flask via a syringe, and the mixture was stirred at 50 °C for 10–20 min. A deep-red color was observed. A monomer (5 mmol) dissolved in 3 mL of NMP (*M1*:*M2*, *M3*, or *M4* was 4.5:0.5 mmol) was added via a syringe. The mixture was stirred at 75 °C for 4 h. The resulting mixture was cooled, and then poured in 10% HCl/acetone to precipitate a polymer. The polymer was collected by filtration, washed with acetone, and dried at 80 °C for 24 h under reduced pressure to give a product in 90% yield.

## 2.5. Preparation of sulfonated SPPs

The postsulfonation of the synthesized copolymers was carried out using concentrated H<sub>2</sub>SO<sub>4</sub> (98%) as the sulfonating agent at room temperature for 72 h.



**Scheme 1.** Chemical structures: (a) candidate monomers and (b) sulfonated copoly(*p*-phenylene)s.

In a typical reaction, 1.0 g of the synthesized copolymers was dissolved in 30 mL of concentrated H<sub>2</sub>SO<sub>4</sub> (96%). The solution was maintained at room temperature for 72 h before inducing precipitation in a large amount of water at room temperature. The sulfonated polymers were filtered, washed thoroughly with deionized water, and dried at 80 °C for 24 h under vacuum. The following results were obtained: FT-IR (KBr) 1653 cm<sup>-1</sup> (C=O), 1586 and 1491 cm<sup>-1</sup> (C=C, aromatic), 1123 and 1031 cm<sup>-1</sup> (asymmetric and symmetric stretching of -SO<sub>3</sub>H).

## 2.6. Membrane preparation

Polymer membranes were prepared by solution casting from DMF. The dried polymer was dissolved in DMF to form a 5% solution, and filtered at room temperature. The membranes were directly casted on a glass plate and dried on a hot plate at 60 °C for 2 h and then at 80 °C in under vacuum for 24 h to give a tough and flexible membrane. The membranes were then immersed in 1 M

HCl at room temperature for 24 h, followed by washing thoroughly with deionized water at room temperature, and dried under vacuum at 100 °C overnight. The thickness of all the membrane samples was in the range of 40–70 μm.

## 2.7. Ion exchange capacity

The ion exchange capacity of the copolymer membranes was determined by a titration method. Polymer membranes in acid form were dried overnight at 100 °C under vacuum, weighed, and immersed in saturated NaCl for 24 h. The amount of H<sup>+</sup> released from the membrane samples was determined by titration with 0.01 M NaOH solution using phenolphthalein as the indicator.

$$\text{IEC} = (C \times V) / M$$

Here, *C* and *V* are the concentration and volume of NaOH, respectively. *M* is the weight of the membrane.

## 2.8. Dimensional change

The dimensional changes of the membranes were measured in the thickness and plane directions by immersing the membrane samples in deionized water at room temperature and 80 °C for a given time. The changes in thickness and length were calculated using

$$\Delta t = (t - t_s)/t_s,$$

$$\Delta l = (l - l_s)/l_s$$

where  $t_s$  and  $l_s$  are the thickness and length of the dry sample, respectively;  $t$  and  $l$  refer to those of the membrane immersed in water for 5 h.

## 2.9. Membrane morphology

Membrane morphology was investigated by atomic force microscopy (JSPM-5400, Nihon Denshi) with a humidity control unit [35]. A Pt-coated cantilever (NSC05/Pt\_20, NT-MDT) with a force constant of 12 Nm<sup>-1</sup> and a resonance frequency of 250 kHz was used. Membrane samples were placed on a gold-plated conductive sample stage with Nafion dispersion (DE-2020, DuPont) as adhesive. Prior to AFM observations, samples were placed in a humidity-controlled chamber for at least 1 h. Bias voltage was applied to the sample stage during AFM. Height and current-mapping images were simultaneously obtained.

## 2.10. Water uptake and proton conductivity

Water uptake and proton conductivity were measured using an isothermal absorption measurement system (MSB-AD-V-FC, BEL Japan, Inc.) equipped with an impedance analyzer (SI 1260, Solartron) with a temperature- and humidity-controlled chamber. Each membrane sample was dried at 80 °C for 2 h under dry nitrogen flow and then exposed to a humidified nitrogen environment at 80 °C. When there was no further weight change of each sample, sample weight and proton conductivity were measured sequentially. Humidity conditions were changed stepwise from 10 to 95% RH. The system used enabled the simultaneous measurements of water uptake and proton conductivity in the same chamber.

The water uptake of the membranes was calculated as

$$\text{Water volume fraction}(V_{f_{H_2O}}) = (W_{\text{wet}} - W_{\text{dry}})/d_{H_2O}/V_{\text{dry}}$$

where  $W_{\text{wet}}$  and  $W_{\text{dry}}$  are the weights of the wet and dry membranes, respectively.  $V_{\text{dry}}$  is the volume of the dry membranes, and  $d_{H_2O}$  is the water density (1 g/cm<sup>3</sup>).

Proton conductivity was measured using a four-point probe AC impedance method from 10 to 100 kHz. The results were collected by Z-view and analyzed using Z-plot software. Proton conductivity was calculated from dry membrane thickness, and membrane resistance was taken at the frequency that produced the minimum imaginary response. Proton conductivity ( $\sigma$ ) was calculated from the impedance data according to the following equation:

$$\sigma = d/A \cdot R,$$

where  $\sigma$  is the proton conductivity,  $d$  is the distance between two electrodes,  $A$  is the membrane cross-sectional area, and  $R$  is the membrane resistance.

## 2.11. Gas permeability

Gas permeability was measured by the equal pressure method with a GTR-Tech 30XFST apparatus equipped with a gas

chromatograph (G2700T, Yanaco) by monitoring the amounts of H<sub>2</sub> and O<sub>2</sub> that permeated across the membrane (dehydrated and stored in dry N<sub>2</sub>), as detailed elsewhere [36]. The relative humidity dependences of H<sub>2</sub> and O<sub>2</sub> permeability coefficients  $P$  were measured from 0 to 90% RH at 80 °C using argon and helium as the carrier gases of H<sub>2</sub> and O<sub>2</sub>, respectively. A 40–70- $\mu$ m-thick membrane was set in a cell with a gas inlet and a gas outlet, where temperature was controlled. H<sub>2</sub> and O<sub>2</sub> were supplied at a flow rate of 30 mL/min. The gas permeability coefficient  $P$  (cm<sup>3</sup> (STP) cm cm<sup>-2</sup> s<sup>-1</sup> cmHg<sup>-1</sup>) was calculated according to the following equation:

$$P = \frac{273}{T} \times \frac{1}{A} \times d \times \frac{1}{76 - P_{H_2O}} \times V \times \frac{60}{B} \times \frac{C}{10^6}$$

where  $T$  (K) is the absolute temperature of the cell,  $A$  (cm<sup>2</sup>) is the permeation area,  $V$  is the sampling tube volume (cm<sup>3</sup>; 4.03 for H<sub>2</sub> and 4.17 for O<sub>2</sub>)  $B$  (cm<sup>3</sup>/min) is the flow rate of the test gas,  $C$  is the volume of gas (cm<sup>3</sup>) that permeated through the membrane as evaluated by the absolute calibration method,  $d$  (cm) is the thickness of the membrane, and  $P_{H_2O}$  (cmHg) is the water vapor pressure.

## 3. Results and discussion

### 3.1. Monomer and polymer synthesis

The chemical structure of the monomer considered here is shown in Scheme 1. All monomers prepared in one step by the Friedel-Crafts catalytic reaction of 2,5-dichlorobenzoyl chloride with various benzene derivatives were synthesized according to the literature with some modifications [19,20,32]. The benzene derivatives used as counterparts of 2,5-dichlorobenzoyl chloride in this study were diphenylether, *n*-propylbenzene, *n*-dodecylbenzene, or *n*-octadecylbenzene. The yield of the final product was approximately 85–95% based on benzene derivatives. The structure of monomers was confirmed by NMR spectroscopy.

As shown in Scheme 1, a series of copolymers with alkyl pendant chains of different lengths (i.e., propyl, dodecyl, and octadecyl) were prepared. Copolymers (PPs) were synthesized by Ni(0)-catalyzed coupling polymerization of 2,5-dichloro-4-phenoxybenzophenone (*M1*) with 2,5-dichloro-4-propylbenzophenone (*M2*), 2,5-dichloro-4-dodecylbenzophenone (*M3*), or 2,5-dichloro-4-octadecylbenzophenone (*M4*), respectively, in NMP in the presence of Ni(PPh<sub>3</sub>)<sub>2</sub>Cl<sub>2</sub>, Zinc powder and triphenylphosphine at 75 °C for 4 h in a similar synthetic method as described in references [32,33]. The molar ratio of *M1* to either of the alkyl side-chain monomers (*M2*, *M3*, and *M4*) was controlled to be 90:10 to provide a reasonably high degree of sulfonation of the synthesized copolymers. The resulting copolymers (PPs) were soluble in various organic solvents, such as dichloromethane, chloroform and DMF. Polymer PPs were then sulfonated with 96% concentrated H<sub>2</sub>SO<sub>4</sub> at room temperature for 3 days, as described in experimental section. After purification and drying, sulfonated copolymers were isolated in yields higher than 90%. All sulfonated copolymers showed solubilities differ from those of the parent PPs. They were highly soluble in polar aprotic solvents such as DMAC, NMP, DMSO, and DMF at room temperature but insoluble in less polar solvents such as chloroform and dichloromethane as a result of the increased hydrophilicity by the introduction of sulfonic acid groups. The molecular weight of each sulfonated polymer was determined by GPC using polystyrene as the standard. As shown in Table 1, the number-average molecular weight ( $M_n$ ) of SPP-1, SPP-2, and SPP-3 was 3.91 × 10<sup>4</sup>, 5.92 × 10<sup>4</sup>, and 4.44 × 10<sup>4</sup>, respectively. Sulfonation of SPPs was confirmed by FT-IR spectra, a convenient method that was used to identify the sulfonic acid group. An example of FT-IR

**Table 1**

Molecular weights, IECs, water uptakes, proton conductivities and dimensional changes of SPP membranes.

Ionomer	$M_n \times 10^4$ (g/mol) <sup>a</sup> ( $M_w/M_n$ )	IEC <sup>b</sup> (mequiv/g)	WU <sup>c</sup> (vol%)	$\lambda^c$	$\sigma$ (S/cm) <sup>d</sup>		Dimensional change			
							RT		80 °C	
							50% RH	95% RH	$\Delta t$	$\Delta l$
SPP-1	3.91(2.8)	2.53	55.7	8.7	0.020	0.271	0.18	0.09	0.37	0.12
SPP-2	5.92(3.8)	2.65	56.4	9.4	0.017	0.284	0.26	0.04	0.39	0.05
SPP-3	4.44(3.8)	2.50	52.2	7.3	0.017	0.208	0.36	0.07	0.54	0.11
SPEEK	–	2.07	41.8	7.7	0.001	0.130	0.32	0.16	– <sup>e</sup>	– <sup>e</sup>
Nafion112	–	0.91	30.1	8.1	0.029	0.127	0.008	0.07	0.02	0.14

<sup>a</sup> Determined by GPC based on polystyrene standards.<sup>b</sup> Measured by titration with 0.01 M NaOH.<sup>c</sup> Measured at 80 °C and 95% RH.<sup>d</sup> At 80 °C.<sup>e</sup> Dissolved.

spectrums of SPPs in comparison with parent polymer (non-sulfonated polymer) was depicted in Fig. 1. The IR spectra of SPPs showed characteristic absorptions due to the carbonyl and ether groups at around 1653 and 1240  $\text{cm}^{-1}$ , respectively. In addition, the new absorption bands at around 1123 and 1031  $\text{cm}^{-1}$  assigned as the symmetric stretching and asymmetric S=O stretching of the sulfonic acid groups in SPPs were observed for all copolymers, indicating the existence of sulfonic acid groups in SPPs. Since SPPs showed good solubility, thin films could be readily prepared by casting from DMF solution. SPP membranes were transparent, flexible, and easy to handle even in their water-swollen or dry form, as opposed to the non-aliphatic membranes containing poly(*p*-phenylene)s which were rather brittle or difficult to be made flexible by casting [18–20]. We speculate that the long alkyl chains in copolymers disrupted the polymer chain–chain interaction (aggregation) and increased the mobility of polymer chains. The most noticeable feature of the copolymers was their ability to form more flexible and ductile films, even in hot water (90 °C), compared with sulfonated poly(4-phenoxybenzoyl-1,4-phenylene)s, (SPPBPs) or SPEEK of the same molecular weight range and IEC value, which broke into pieces or dissolved in hot water at 90 °C.

### 3.2. Membrane stability

The thermal stability of non-sulfonated (PPs) and sulfonated copolymers (SPPs) was determined by thermogravimetric analysis (TGA) at a heating rate of 10 °C/min in nitrogen or air atmosphere. The non-sulfonated polymers (PPs) showed excellent thermal

stability as shown in Fig. 2. PPs showed single step degradation with 5% weight loss temperature above 500 °C. However, in the TGA curves of sulfonated copolymers (SPPs) (Fig. 3), a two-step weight loss profile was observed. All polymers displayed a similar weight loss behavior, which differed slightly in terms of total percentage weight loss. The first-stage weight loss around 250–400 °C was caused by the decomposition of the sulfonic acid and alkyl moieties. The second-stage weight loss appearing at around 500 °C was attributed to the main-chain decomposition. Surprisingly, however, those polymers exhibited almost the same thermal stability in air as that in N<sub>2</sub> atmosphere in the ranging from 220 to 400 °C caused by the decomposition of the sulfonic acid. This indicates that degradation of SPPs in air had no significant effect on the thermal stability of the sulfonic group on the polymer side chain. However, the third-stage weight loss related to the degradation of the main chain of SPP was faster under air atmosphere than nitrogen atmosphere in the temperature range of 410–550 °C.

Moreover, breaking strength and elongation at break point under humidified condition were also investigated. The breaking strength of SPP-1 and SPP-2 was 26 and 30 MPa, respectively, at 90% RH and 80 °C. Although there is no marked difference in breaking strength between SPP-1 and SPP-2, there was a significant difference in elongation at break point: 17% for SPP-1 and 40% for SPP-2. This significant difference indicates that a longer alkyl side chain of the copolymer system can effectively contribute to structural stabilization, particularly for membrane flexibility even for membranes with higher water content. This result implies that a longer alkyl side chain can participate in the enhancement of intermolecular interaction resulting in mechanical stability.

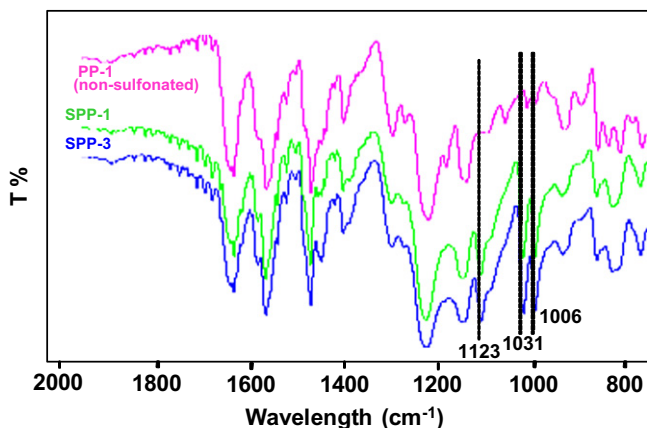
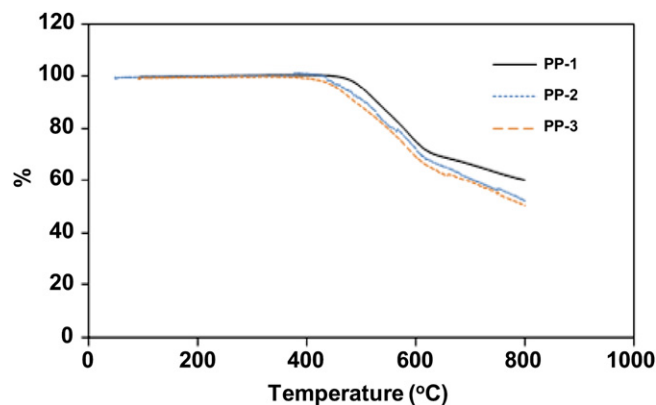


Fig. 1. FT-IR spectra of non-sulfonated PP-1 and sulfonated SPP-1 and SPP-3.

Fig. 2. TGA thermograms of PPs (before sulfonation) under N<sub>2</sub> atmosphere.

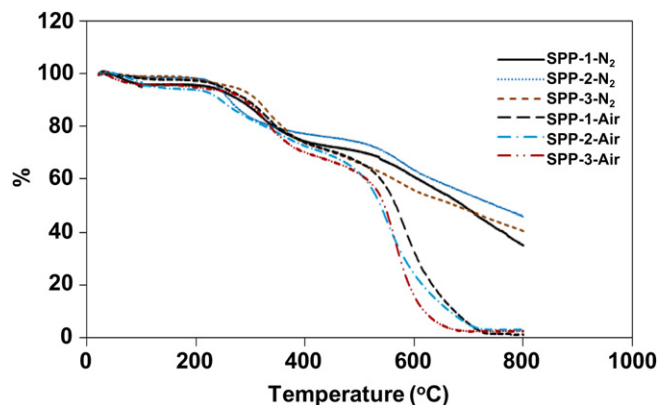


Fig. 3. TGA thermograms of SPPs (postsulfonation) under N<sub>2</sub> and air atmosphere.

### 3.3. Membrane morphology

The membrane morphology of SPPs was examined by AFM. Fig. 4 shows AFM topographic images of SPP-1 under controlled humidity (50% RH and 85% RH) at room temperature. In Fig. 4, noodle-like structures were observed. With increasing relative humidity, the structures became thicker and clearly distinguished from each other owing to swelling, as shown in the height image. Fig. 5 shows topographic and current-mapping AFM images of SPP-1 and SPP-2 taken under 85% RH. A correlation between height and current-mapping images was hardly found in either membrane. A darker region, which corresponded to a proton conduction area, was found to be distributed and each domain size was approximately 10–20 nm in both membranes. From the height images, it has been found that SPP-2 has a more microscopic structure than SPP-1. Several 10-nm-scale particles can be seen in Fig. 5C. It is thought that the slightly weakened interaction between phenylene main chains with the introduction of a longer alkyl side chain facilitates the development of a microscopic structure. In both current-mapping images in Fig. 5B and D, the size of the conduction areas is only slightly different; a proton conduction area is well distributed in each membrane. This morphological feature is consistent with the result of proton conductivity measurement in bulk, and this is expected because a random copolymer system with a relatively higher IEC can more easily form a less phase-segregated and distributed hydrophilic domain.

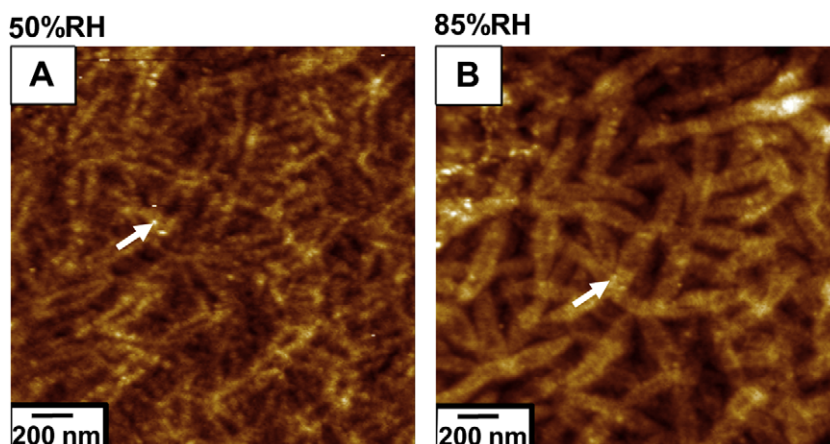
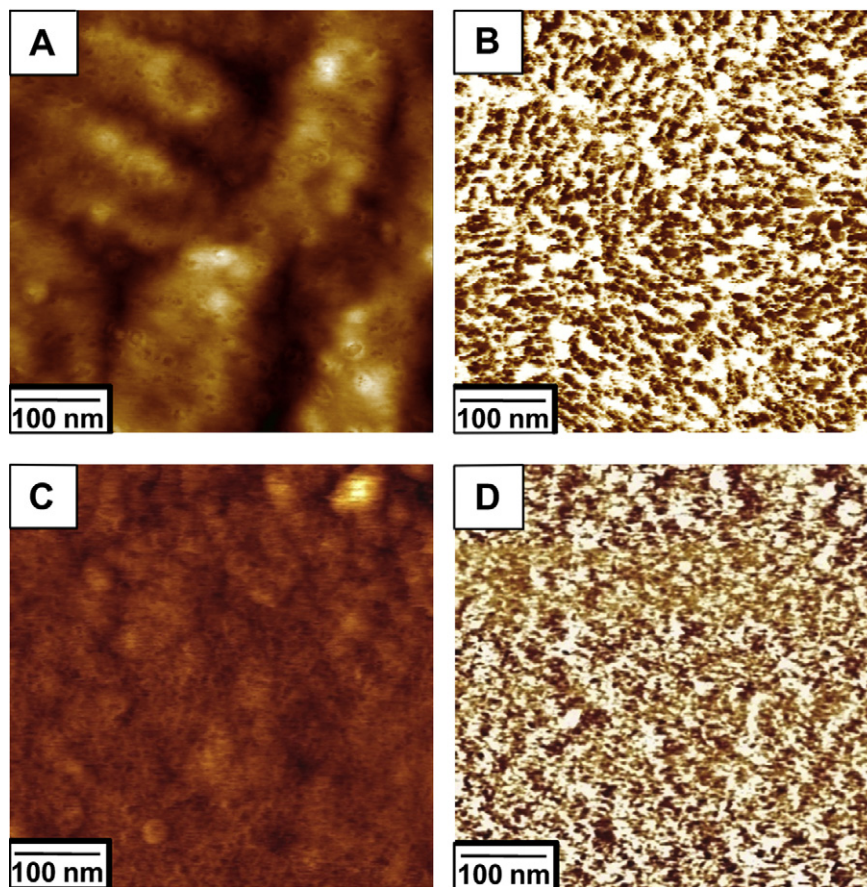


Fig. 4. AC-AFM height images of SPP-1 at 50% and 85% relative humidity. z-Scale maximum: (A) 11 nm, (B) 16 nm; scan size: 2  $\mu\text{m}$   $\times$  2  $\mu\text{m}$ ; scan rate: 1 Hz; and applied bias voltage:  $-1.6$  V. For comparison, in both images, the same structure (marked by white arrow) was observed.

Concerning the chain conformation in the membrane, the UV–vis absorption spectra of SPPs in DMF solution and thin film states were studied. In Fig. 6, the chain conformation corresponding to the observed absorbance at 294 nm in solution state markedly changed to a lower-energy band at approximately 380–395 nm in solid state, due to a rigid-rod conformation that possesses a much larger and uniform conjugation length in solid state. The coplanar conformation of the main chain backbone might be favored, resulting in the extension of the conjugation length in the membrane. Furthermore, although chain conformation seems to be independent of the chain length of aliphatic alkyl side chain in solution state, some differences were seen among SPP-1 (propyl), SPP-2 (dodecyl), and SPP-3 (octadecyl) membranes. The wavelength ( $\lambda_{\text{max}}$ ) of SPP-3 was 15 nm shorter than that of SPP-1 and SPP-2. The steric hindrance of the longest alkyl (C18) side chain of SPP-3 may prevent the main chain perturbation from forming a uniform conformation, while the C12 side chain does not readily affect the chain conformation of the backbone.

### 3.4. Water uptake and proton conductivity

The water uptake (vol%) of SPP membranes was measured as a function of humidity (10–95% RH) at 80 °C and compared with that of the Nafion membrane. As shown in Fig. 7A, SPP membranes exhibited higher water uptake values than Nafion in the entire relative humidity range (10–95% RH) owing to their higher IEC values. When the relative humidity increased from 50 to 95% RH, water uptake further increased. This may be because of the formation of a large and continuous ion network in sulfonated polymers. Water uptake also results in dimensional changes in membrane thickness and in-plane direction, as determined by comparing hydrated membranes with dry membranes. In general, membranes fabricated from polymers with poor hydrophilic–hydrophobic balance display a marked increase in lateral dimensions upon hydration, particularly those with a higher IEC. However, although their water uptake is relatively high SPP copolymers that had short or long aliphatic alkyl side chains showed small in-plane and through-plane dimensional changes. From the results shown in Table 1, SPPs displayed anisotropic membrane swelling and exhibited much (2–3 times) larger swelling in the membrane thickness direction than in the plane direction. This may have resulted from some effects of the aliphatic alkyl chain that allowed the relaxation of polymer chain within a small dimensional change. It should be emphasized here that



**Fig. 5.** AC-AFM height images of SPPs at 85% RH: (A, C) Topography: z-scale maximum: (A) SPP-1: 13 nm, (C) SPP-2: 7 nm (B, D) Current-mapping images: z-scale maximum: (B) SPP-1: 50 pA and (D) SPP-2: 40 pA. Scan size: 500 nm × 500 nm. Scan rate: 1 Hz. Applied bias voltage: −1.6 V.

even though SPPs have a high water content, their dimensional change is significantly small compared with that of SPEEK and SPPBP. This result indicates that an alkyl side chain in a copolymer can contribute to the prevention of membrane deformation by swelling. This behavior is also promising because the low in-plane swelling may result in a much lower stress at the interface and better stability of the membrane electrode assembly (MEA) [37].

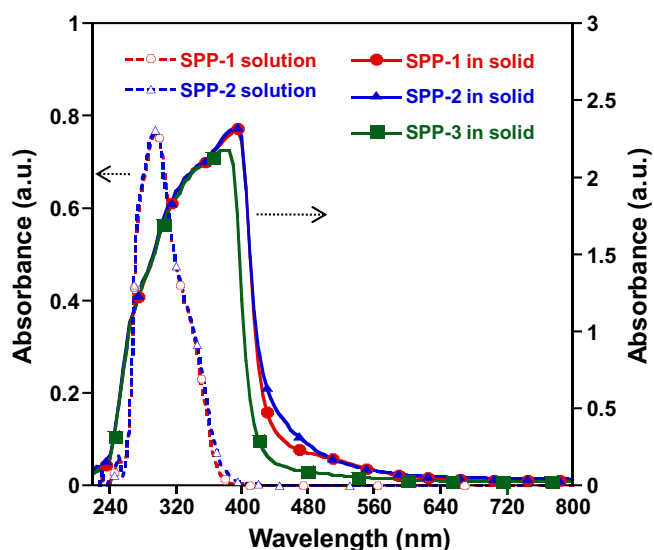


**Fig. 6.** UV-vis absorption spectra of SPPs in DMF (with 10 mM LiBr) and solid film at room temperature.

Proton conductivity at 80 °C and different relative humidity were also measured. For comparison, the conductivity of Nafion was obtained under the same conditions. Fig. 7B shows the relative humidity dependence of proton conductivity for SPP membranes and Nafion at 80 °C. The conductivity at 50, 70 and 95% RH at 80 °C is also listed in Table 1. The SPP membranes generally displayed a stronger RH dependence of conductivity than Nafion. All SPP membranes exhibited higher conductivity than Nafion in the RH range of 70–95% RH. In comparison, SPP-2 displayed the highest conductivity at 95% RH and the  $\sigma$  values were around 0.284 S/cm, Nafion® (0.127 S/cm, 95% RH) under the same measurement conditions. The number of water molecules per sulfonic group ( $\lambda$ ) is also listed in Table 1. The  $\lambda$  values of SPP membranes increased as relative humidity increased. Despite the increase in water content with IEC, there was no significant difference in  $\lambda$  between SPPs and Nafion. For Nafion, continuous water channels can be formed even with a small amount of water, but for SPEEK, a less phase-separated structure cannot incorporate sufficient water. Less chain mobility prevented the formation of a large water domain in the membrane. For SPPs, however, their  $\lambda$  values were similar to those of Nafion. This result implies that SPPs can form a larger water domain. Our AFM current-mapping images also clearly show that SPPs have conductive domains approximately 10–20 nm in size, whereas SPEEK has small conductive domains less than 10 nm in size [35].

### 3.5. Hydrogen and oxygen permeabilities

Since the crossover of hydrogen ( $H_2$ ) and oxygen ( $O_2$ ) between the anode and cathode in MEA has a negative impact on the efficiency of PEFC, the PEM should be a good gas barrier. Fig. 8 shows the humidity

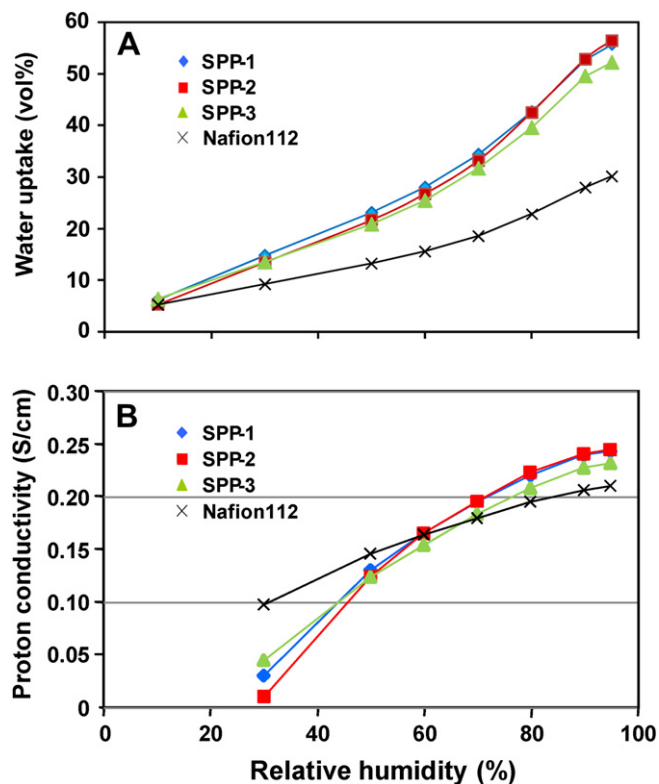


Fig. 7. Relative humidity dependence of (A) water uptake and (B) proton conductivity of *SPP* membranes compared with those of Nafion 112 at 80 °C.

dependences of  $H_2$  and  $O_2$  permeability of *SPP* membranes and Nafion at 80 °C. Both  $H_2$  and  $O_2$  permeability of *SPP* membranes are smaller than those of Nafion ( $P_{H_2}$  of *SPP-1*, *SPP-2*, *SPP-3* and Nafion at 80 °C, 85% RH:  $2.17 \times 10^{-9}$ ,  $1.87 \times 10^{-9}$ ,  $2.24 \times 10^{-9}$  and  $6.88 \times 10^{-9}$   $\text{cm}^3$  (STP)  $\text{cm}^{-2} \text{s}^{-1} \text{cmHg}^{-1}$ , respectively, and  $P_{O_2}$  of *SPP-1*, *SPP-2*, *SPP-3* and Nafion at 80 °C, 85% RH:  $6.93 \times 10^{-10}$ ,  $4.76 \times 10^{-10}$ ,  $6.27 \times 10^{-10}$  and  $2.66 \times 10^{-9}$   $\text{cm}^3$  (STP)  $\text{cm}^{-2} \text{s}^{-1} \text{cmHg}^{-1}$ , respectively.). Although a small difference in  $H_2$  permeability can be seen at a lower RH, the overall permeability is almost the same among the three membranes *SPP-1*, *SPP-2* and *SPP-3*. However, the  $O_2$  permeation behavior of *SPP-1* is significantly different from that of *SPP-2* and *SPP-3* during hydration. The  $O_2$  permeability of *SPP-1* increased with water uptake, but in the case of *SPP-2* and *SPP-3* decreased with increasing relative humidity from 0 to 10% RH. Above 10% RH, an increase in permeability was clearly observed. These differences are related to the length of the aliphatic alkyl side chain in *SPP* copolymers. The decrease in permeability with decreasing humidity might have been caused by water molecules filling free-volume holes as a result of stabilized intermolecular interaction, and the increase in permeability with increasing humidity is caused by the plasticizing effect of water molecules, as can be seen in the case of *SPP-2* and *SPP-3*. Similar permeation behavior has been reported for ethylene–vinyl alcohol copolymer (EVOH) by Muramatsu et al. [38]. Since *SPP-3* has a larger free volume due to having the longest alkyl side chain (larger van der Waals radii), its permeability is higher than that of *SPP-2*, although a stronger intermolecular interaction may occur in its membrane. For *SPP-1*, it is not unambiguous at the present why *SPP-1* showed different permeation behavior at low RH from *SPP-2* and *SPP-3*. Since the permeability coefficient ( $P$ ) is expressed by product of diffusivity ( $D$ ) and solubility ( $S$ ) parameters ( $P = DS$ ) both parameters could be changed during hydration. Further study will be needed for the clarification.

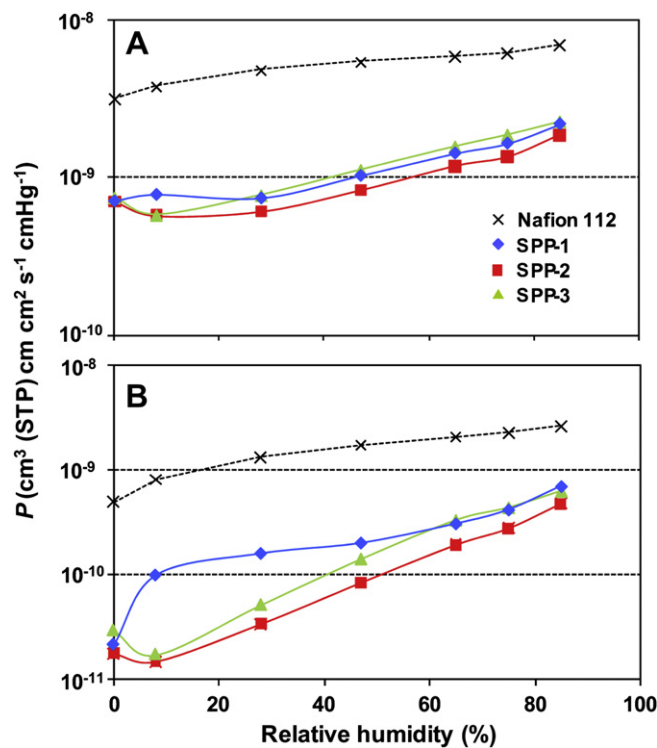


Fig. 8. Permeability of (A)  $H_2$  and (B)  $O_2$  as functions of relative humidity of *SPP* membranes at 80 °C.

#### 4. Conclusion

A series of novel copoly(*p*-phenylene) containing pendant aliphatic alkyl groups were synthesized via Ni(0)-catalyzed coupling polymerization from 2,5-dichloro-4-phenoxybenzophenone with aromatic dichloride containing an aliphatic propyl, *n*-dodecyl, or *n*-octadecyl side chain. The synthesized polymers readily dissolved in water temperature in aprotic polar solvents such as DMF, DMSO, and NMP and formed tough, transparent and flexible films by solution casting. All the polymers showed excellent proton conductivity and good dimensional stability at high temperatures. The gas permeability of the *SPP* membranes was lower than that of Nafion 112. The incorporation of an aliphatic alkyl side chain into copolymers improved the properties of the polymers such as solubility, flexibility, and film-forming ability and reduced swelling in water at enhanced temperatures compared to other sulfonated poly(*p*-phenylene)s. We would like to emphasize here that introducing an aliphatic alkyl pendant chain confers significant dimensional stability but does not lead to the loss of other significant properties such as proton conductivity and the ability to serve as a gas barrier.

Thus, we have demonstrated that significant performance such as higher proton conductivity and good ability to serve as a gas barrier with dimensional stability can be optimized by a simple and easy means, that is, by the introduction of an aliphatic alkyl pendant chain. The *SPP* membranes synthesized here can be considered promising alternative PEM materials for fuel cell application, although further improvement is required for their practical use.

#### Acknowledgements

This work was financially supported by the Ministry of Economy, Trade and Industry (METI) and the New Energy and Industrial Technology Development Organization (NEDO), Japan.

We are grateful to Prof. Rikukawa of Sophia University for providing the sulfonated poly(4-phenoxybenzoyl-1,4-phenylene)s (SPPBPs).

## References

- [1] Hickner MA, Ghassemi H, Kim Y, Einsla B, McGrath JE. *Chem Rev* 2004;104:4587.
- [2] Mauritz K, Moor R. *Chem Rev* 2004;104:4535.
- [3] Rikukawa M, Sanui K. *Prog Polym Sci* 2000;25:1463.
- [4] Miyake K, Zhou H, Matsuo T, Uchida H, Watanabe M. *Macromolecules* 2004;37:4961.
- [5] Piroux F, Espuche E, Mercier R. *J Membr Sci* 2004;232:115.
- [6] Zhai F, Guo X, Fang J, Xu H. *J Membr Sci* 2007;296:102.
- [7] Guo X, Fang J, Watari T, Tanaka K, Kita H, Okamoto K. *Macromolecules* 2002;35:6707.
- [8] Linkous CA, Anderson HR, Kopitzke RW, Nelson GL. *Int J Hydrogen Energy* 1998;23:525.
- [9] Xing P, Robertson GP, Guiver MD, Mikhailenko SD, Wang K, Kaliaguine S. *J Membr Sci* 2004;229:95.
- [10] Zhang G, Fu T, Shao K, Li X, Zhao C, Na H, et al. *J Power Sources* 2009;189:875.
- [11] Matsumura S, Hlil AR, Lepiller C, Gaudet J, Guay D, Shi Z, et al. *Macromolecules* 2008;41:281.
- [12] Miyake K, Chikashige Y, Higuchi E, Watanabe M. *J Am Chem Soc* 2007;129:3879.
- [13] Kim DS, Shin KH, Park HB, Chung YS, Nam SY, Lee YM. *J Membr Sci* 2006;278:428.
- [14] Nolte R, Ledjeff K, Bauer M, Mulbaupt R. *J Membr Sci* 1993;83:211.
- [15] Roy A, Lee HS, McGrath JE. *Polymer* 2008;49:5037.
- [16] Asensio JA, Gomez-Romeo P. *Fuel Cells* 2005;5:336.
- [17] Kobayashi T, Rikukawa M, Sanui K, Ogata N. *Solid State Ionics* 1998;106:219.
- [18] Ghassemi H, McGrath JE. *Polymer* 2004;45:5847.
- [19] Hickner MA, Fujimoto CH, Cornelius CJ. *Polymer* 2006;47:4238.
- [20] Cherry BR, Fujimoto CH, Cornelius CJ, Alam TM. *Macromolecules* 2005;38:1201.
- [21] Fujimoto CH, Hickner MA, Cornelius CJ, Loy DA. *Macromolecules* 2005;38:5010.
- [22] Li Q, Pan C, Jensen JO, Noy P, Bjerrum N. *Chem Mater* 2007;19:350.
- [23] Jorissen L, Gogel V, Kerres J, Garcke J. *J Power Sources* 2002;105:267.
- [24] Fang J, Zhai F, Guo X, Xu H, Okamoto K. *J Mater Chem* 2007;17:1102.
- [25] Buchi FN, Gupta B, Haas O, Scherer GG. *Electrochimica Acta* 1995;40:345.
- [26] Kabanov VY. *High Energy Chem* 2004;38:57.
- [27] Nakabayashi K, Matsumoto K, Ueda M. *J Polym Sci Part A Polym Chem* 2008;46:3947.
- [28] Genies C, Mercier R, Sillion B, Cornet N, Gebel G, Pineri M. *Polymer* 2001;42:359.
- [29] Ghassemi H, Ndip G, McGrath JE. *Polymer* 2004;45:5855.
- [30] Lee HS, Badami AS, Roy A, McGrath JE. *J Polym Sci Part A Polym Chem* 2007;45:4879.
- [31] Chang JH, Park JH, Park GG, Kim CS, Park OO. *J Power Sources* 2003;124:18.
- [32] Wang J, Sheares V. *Macromolecules* 1998;31:6769–75.
- [33] Hagberg E, Olson D, Sheares V. *Macromolecules* 2004;37:4748–58.
- [34] Northop BH, Glockner A, Stang PJ. *J Org Chem* 2008;73:1787.
- [35] Takimoto N, Wu L, Ohira A, Takeoka Y, Rikukawa M. *Polymer* 2009;50:534.
- [36] Asano N, Aoki M, Suzuki S, Miyatake K, Uchida H, Watanabe M. *J Am Chem Soc* 2006;128:1762.
- [37] Roy A, Yu X, Dum S, McGrath JE. *J Membr Sci* 2009;327:118.
- [38] Muramatsu M, Okura M, Kuboyama K, Ougizawa T, Yamamoto T, Nishihara Y, et al. *Radiat Phys Chem* 2003;68:561.